

Adaptive Neural Network Control for Load-Varying Two-Link Robots Using Honey Badger Optimization

Kareem Al-Badri ^{1*}, Hussien Dulaimi ², Huthaifa Al-Khazraji ³, Amjad J Humaidi ⁴

^{1, 2, 3, 4} Control and Systems Engineering Department, University of Technology - Iraq, Al-Sina'a Street, Baghdad 10066, Iraq
Email: ¹ 60186@uotechnology.edu.iq, ² 60179@uotechnology.edu.iq, ³ 60141@uotechnology.edu.iq,

⁴ amjad.j.humaidi@uotechnology.edu.iq

*Corresponding Author

Abstract—This paper illustrates a proportional-integral-derivative based neural network (PID-NN) controller to manipulate the angular position of the two-link robot considering the load variation on the system. The two-link robot system's dynamic equations were derived using the Lagrange method. To improve the tuning process of the design coefficients of the controller, the learning process was framed as an optimization task. Subsequently, to determine the optimal weight values, the honey badger algorithm (HBA) was introduced. To analyze how well the proposed controller performs, Simulations in MATLAB were carried out to compare the PID-NN controller against a PI-PD controller. The findings revealed superior performance of the PID-NN controller in standard conditions. Furthermore, the PID-NN demonstrated a substantial enhancement when a load variation was augmented.

Keywords—Robotic Manipulators; Neural Network Controller; PID Controller; PI-PD; Honey Badger Algorithm.

I. INTRODUCTION

A key element of the current manufacturing sector is the two-link robot arm system [1]. Furthermore, people who have trouble doing physical tasks can benefit from the medical use of robotic arms [2]. Such multi-input multi-output (MIMO) system is strongly linked, nonlinear, and has time-dependent behaviors. The uncertainties brought on by the unknown loads that the robot arm must manage (such as pick and place jobs) are one of the main obstacles to using the robot arm structure with two connections [3]. Regarding control design, the two-link robot arm system is a double pendulum system, where the Lagrange equation can be used to determine the equation of motion [4]. In addition to its complicated nonlinear framework, the two-link robot arms model can be utilised as a reference framework for evaluating and testing numerous control techniques [5].

In particular, Guechi et al. compared the performance of two distinct control strategies—Linear Quadratic (LQ) control and Model Predictive Control (MPC) after applying feedback linearization to a two-link robotic arm [6]. It has been noted that the MPC control strategy performs better than the LQ control approach. Similarly, Mohammed and Eltayeb [5] explored how dependable Sliding Mode Control (SMC) is when compared to a conventional PID-based approach. The results of this investigation showed that the SMC's performance is more robust and responds more quickly than

the PID controllers. However, SMC discovered a superior control signal. The fuzzy logic controller (FLC) was used by [2] as an alternate control method. A robust PID controller was proposed by Baccouch and Dodds [1]. Bendimrad [7] recently presented an SMC method for two-link robot arm control. Long et al. [8] introduced a dynamic framework PID control technique for the two-link robotic arm system, utilizing the robustness of the SMC and the straightforward structure of the PID. The results demonstrate that the suggested strategy maintained the same steady-state accuracy while increasing the rate of convergence by over 80% when compared to the traditional PID control method. Shen [9] suggested a Fuzzy Neural Network (FNN) controller as an intelligence controller. The provided control design parameters have been optimised using the backpropagation (BP) approach and particle swarm optimisation (PSO). Applying the control structure, the research findings illustrate that the system has outstanding detecting efficiency, adaptability, and robustness.

Unlike previous studies, this research combines two advanced control methods for the two-link robotic system: a neural network governed by PID logic and a PI-PD scheme that separates integral and derivative actions. The PID-NN and PI-PD controllers can be thought of as upgraded versions of the classical PID controller. Different swarm optimization techniques have been presented in the literature to obtain an optimal performance of the controllers, as compared to finding the accurate value of each controller modified configurations by trail and error. The ability to solve multivariate, high-dimensional engineering problems has significantly improved because to swarm optimization techniques, which are very simple to use [10]–[23]. In order to adjust the two controllers according to the error performance index, this work presents the honey badger algorithm (HBA).

This paper subsequently is divided into several sections: Section 2 defines the basic concept of the two-link robotic arm system. Section 3 reviews the suggested control methods, and Section 4 provides details on the Honey Badger Optimization technique. Section 5 analyzes and discusses the simulation outcomes. Finally, Section 6 provides concluding remarks and findings.



II. MATHEMATICAL MODEL

This section covers in-depth description of the two-link robot technique mathematical structure. The system can be simplified to a dual pendulum containing two masses, as shown in Fig. 1, M_1 and M_2 , coupled by two rigid, weightless rods of lengths, L_1 and L_2 [1]. The angle that rotates around the origin (θ_1) and the angle that rotates at the first pendulum's endpoint (θ_2) indicate the two degrees of freedom of the two-link robot arm method. The couple input torques (τ_1 and τ_2) control the two angles (θ_1 and θ_2), which are the system's outputs [1].

One needs to initially identify the system Kinetic Energy (KE) and Potential Energy (PE) to be able to execute the Lagrangian approach to formulate the models of motion. This fundamental step in Lagrangian mechanics requires precise determination of these energy components before establishing the dynamic equations.

For the first mass, the equation of the mass in x direction and y direction is given by:

$$x_1 = L_1 \cos(\theta_1) \quad (1)$$

$$y_1 = L_1 \sin(\theta_1) \quad (2)$$

For the second mass, the equation of the mass in x direction and y direction is presented by:

$$x_2 = L_1 \cos(\theta_1) + L_2 \cos(\theta_2) \quad (3)$$

$$y_2 = L_1 \sin(\theta_1) + L_2 \sin(\theta_2) \quad (4)$$

The rate of motion of the two masses is given by:

$$v_1 = \sqrt{\dot{x}_1^2 + \dot{y}_1^2} \quad (5)$$

$$v_2 = \sqrt{\dot{x}_2^2 + \dot{y}_2^2} \quad (6)$$

where:

$$\dot{x}_1 = -L_1 \dot{\theta}_1 \sin(\theta_1) \quad (7)$$

$$\dot{y}_1 = L_1 \dot{\theta}_1 \cos(\theta_1) \quad (8)$$

$$\dot{x}_2 = -L_1 \dot{\theta}_1 \sin(\theta_1) - L_2 \dot{\theta}_2 \sin(\theta_2) \quad (9)$$

$$\dot{y}_2 = L_1 \dot{\theta}_1 \cos(\theta_1) + L_2 \dot{\theta}_2 \cos(\theta_2) \quad (10)$$

The Lagrangian equation is presented by:

$$L = KE - PE \quad (11)$$

The kinematic energy of the system can be obtained as follows:

$$KE = \frac{1}{2} M_1 v_1^2 + \frac{1}{2} M_2 v_2^2 \quad (12)$$

Substitute v_1 and v_2 as given in Eq. (5) and Eq. (6) respectively yields:

$$KE = \frac{1}{2} M_1 (\dot{x}_1^2 + \dot{y}_1^2) + \frac{1}{2} M_2 (\dot{x}_2^2 + \dot{y}_2^2) \quad (13)$$

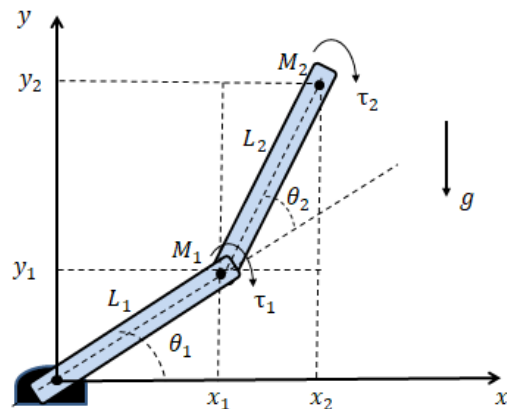


Fig. 1. Double-link robot arm framework

Substitute $\dot{x}_1, \dot{y}_1, \dot{x}_2$ and \dot{y}_2 as given in Eqs. (7) – (10), the KE can be rewritten as:

$$KE = \frac{1}{2} M_1 \left((-L_1 \dot{\theta}_1 \sin(\theta_1))^2 + (L_1 \dot{\theta}_1 \cos(\theta_1))^2 \right) + \frac{1}{2} M_2 \left((-L_1 \dot{\theta}_1 \sin(\theta_1) - L_2 \dot{\theta}_2 \sin(\theta_2))^2 + (L_1 \dot{\theta}_1 \cos(\theta_1) + L_2 \dot{\theta}_2 \cos(\theta_2))^2 \right) \quad (14)$$

Eq. (14) can be rearranged as follows:

$$KE = \frac{1}{2} (M_1 + M_2) L_1^2 \dot{\theta}_1^2 + \frac{1}{2} M_2 L_2^2 \dot{\theta}_2^2 + M_2 L_1 L_2 \dot{\theta}_1 \dot{\theta}_2 \cos(\theta_1 - \theta_2) \quad (15)$$

The following explains the potential energy:

$$PE = M_1 g y_1 + M_2 g y_2 \quad (16)$$

Substitute y_1 and y_2 as given in Eq. (2) and Eq. (4) respectively obtains:

$$PE = M_1 g (L_1 \sin(\theta_1)) + M_2 g (L_1 \sin(\theta_1) + L_2 \sin(\theta_2)) \quad (17)$$

Eq. (17) can be simplified as:

$$PE = (M_1 + M_2) g L_1 \sin(\theta_1) + M_2 g L_2 \sin(\theta_2) \quad (18)$$

Substitute Eq. (15) and Eq. (18) into Eq. (11)

$$L = \left(\frac{1}{2} M_1 \left((-L_1 \dot{\theta}_1 \sin(\theta_1))^2 + (L_1 \dot{\theta}_1 \cos(\theta_1))^2 \right) + \frac{1}{2} M_2 \left((-L_1 \dot{\theta}_1 \sin(\theta_1) - L_2 \dot{\theta}_2 \sin(\theta_2))^2 + (L_1 \dot{\theta}_1 \cos(\theta_1) + L_2 \dot{\theta}_2 \cos(\theta_2))^2 \right) - ((M_1 + M_2) g L_1 \sin(\theta_1) + M_2 g L_2 \sin(\theta_2)) \right) \quad (19)$$

The following is the outcome to the Euler-Lagrange formula:

$$\frac{d}{dt} \left[\frac{\partial L}{\partial \dot{\theta}_i} \right] - \frac{\partial L}{\partial \theta_i} = \tau_i, i = 1, 2 \quad (20)$$

The partial derivatives of Eq. (20) w.r.t to $i = 1$ obtains:

$$\frac{\partial L}{\partial \dot{\theta}_1} = (M_1 + M_2) L_1^2 \dot{\theta}_1 + M_2 L_1 L_2 \dot{\theta}_2 \cos(\theta_1 - \theta_2) \quad (21)$$

$$\frac{\partial L}{\partial \theta_1} = -M_2 L_1 L_2 \dot{\theta}_1 \dot{\theta}_2 \sin(\theta_1 - \theta_2) - (M_1 + M_2) g L_1 \cos(\theta_1) \quad (22)$$

Then:

$$\frac{d}{dt} \left[\frac{\partial L}{\partial \dot{\theta}_1} \right] = (M_1 + M_2) L_1^2 \ddot{\theta}_1 + M_2 L_1 L_2 \ddot{\theta}_2 \cos(\theta_1 - \theta_2) - M_2 L_1 L_2 \dot{\theta}_2 (\dot{\theta}_1 - \dot{\theta}_2) \sin(\theta_1 - \theta_2) - \theta_2 \quad (23)$$

Substitute Eq. (22) and Eq. (23) into Eq. (20) w.r.t $i = 1$ obtains:

$$\begin{aligned} & ((M_1 + M_2) L_1^2 \ddot{\theta}_1 + M_2 L_1 L_2 \ddot{\theta}_2 \cos(\theta_1 - \theta_2) \\ & - M_2 L_1 L_2 \dot{\theta}_2 (\dot{\theta}_1 - \dot{\theta}_2) \sin(\theta_1 - \theta_2) \\ & - ((M_1 + M_2) L_1^2 \dot{\theta}_1 \\ & + M_2 L_1 L_2 \dot{\theta}_2 \cos(\theta_1 - \theta_2)) = \tau_1 \end{aligned} \quad (24)$$

In the same way, the partial derivatives of Eq. (20) w.r.t $i = 2$ obtains:

$$g_1 = \frac{\frac{M}{M_2} \frac{\tau_1}{L_1} - M L_2 \dot{\theta}_2^2 \sin(\theta_1 - \theta_2) - g \cos(\theta_1) - M \cos(\theta_1 - \theta_2) \left[\frac{\tau_2}{M_2 L_2} + L_1 \dot{\theta}_1^2 \sin(\theta_1 - \theta_2) - g \cos(\theta_2) \right]}{L_1 (1 - M \cos^2(\theta_1 - \theta_2))} \quad (31)$$

$$g_2 = \frac{\frac{\tau_2}{M_2 L_2} + L_1 \dot{\theta}_1^2 \sin(\theta_1 - \theta_2) - g \cos(\theta_1) - \cos(\theta_1 - \theta_2) \left[\frac{M}{M_2} \frac{\tau_1}{L_1} + M L_2 \dot{\theta}_2^2 \sin(\theta_1 - \theta_2) - g \cos(\theta_1) \right]}{L_2 (1 - M \cos^2(\theta_1 - \theta_2))} \quad (32)$$

$$M = \frac{M_2}{M_1 + M_2} \quad (33)$$

Let x_1 represents θ_1 , x_2 represents θ_2 , x_3 represents $\dot{\theta}_1$ and x_4 represents $\dot{\theta}_2$. The differential equations is the behaviour of the two-link robot arm system:

$$\dot{x}_1 = x_3 \quad (34)$$

$$\dot{x}_2 = x_4 \quad (35)$$

$$\dot{x}_3 = g_1(t, x_1, x_2, x_3, x_4, \tau_1, \tau_2) \quad (36)$$

$$\dot{x}_4 = g_2(t, x_1, x_2, x_3, x_4, \tau_1, \tau_2) \quad (37)$$

III. CONTROLLER DESIGN

In addition to its durability and effectiveness, a conventional PID controller is widely used in control construction [24]-[28]. Many authors developed different structures of the classical PID controller. In this direction, this paper presents designing PID-NN controller, The two-link robot system angular position is capable of controlled using a PI-PD controller. Neural networks have emerged as promising solutions for nonlinear control applications, owing to their inherent adaptive capabilities, ability to handle nonlinear systems, and self-learning properties [29]-[36]. These networks consist of interconnected processing units known as neurons (n), which work together to process information, which are connected with each other via interconnections known as the weights (w) [37]. The

$$\frac{\partial L}{\partial \dot{\theta}_2} = M_2 L_2^2 \dot{\theta}_2 + M_2 L_1 L_2 \dot{\theta}_1 \cos(\theta_1 - \theta_2) \quad (25)$$

$$\frac{\partial L}{\partial \theta_2} = M_2 L_1 L_2 \dot{\theta}_1 \dot{\theta}_2 \sin(\theta_1 - \theta_2) - M_2 g L_2 \cos(\theta_2) \quad (26)$$

$$\frac{d}{dt} \left[\frac{\partial L}{\partial \dot{\theta}_2} \right] = M_2 L_2^2 \ddot{\theta}_2 + M_2 L_1 L_2 \ddot{\theta}_1 \cos(\theta_1 - \theta_2) - M_2 L_1 L_2 \dot{\theta}_1 (\dot{\theta}_1 - \dot{\theta}_2) \sin(\theta_1 - \theta_2) \quad (27)$$

Substitute Eq. (25) and Eq. (26) into Eq. (20) w.r.t $i = 2$ obtains:

$$\begin{aligned} & (M_2 L_2^2 \ddot{\theta}_2 + M_2 L_1 L_2 \ddot{\theta}_1 \cos(\theta_1 - \theta_2) \\ & - M_2 L_1 L_2 \dot{\theta}_1 (\dot{\theta}_1 - \dot{\theta}_2) \sin(\theta_1 - \theta_2) \\ & - (M_2 L_1 L_2 \dot{\theta}_1 \dot{\theta}_2 \sin(\theta_1 - \theta_2) \\ & - M_2 g L_2 \cos(\theta_2)) = \tau_2 \end{aligned} \quad (28)$$

Solving Eq. (24) and Eq. (28) for $\ddot{\theta}_1$ and $\ddot{\theta}_2$ respectively yields:

$$\ddot{\theta}_1 = g_1(t, \theta_1, \theta_2, \dot{\theta}_1, \dot{\theta}_2, \tau_1, \tau_2) \quad (29)$$

$$\ddot{\theta}_2 = g_2(t, \theta_1, \theta_2, \dot{\theta}_1, \dot{\theta}_2, \tau_1, \tau_2) \quad (30)$$

Where (31)(32):

network's weights possess adaptive learning properties that enable them to establish meaningful connections between system inputs and outputs. Optimizing these weight values directly enhances the neural network's overall performance.

A. PID-NN Controller

Three forward layers make up the architecture of the suggested PID-NN controller: the input (n), the hidden (h), and the output (o) layers. Based on the concept of the PID controller, The network's input layer processes three signal components: instantaneous error, its time integral, and time derivative, all using linear activation functions. A hidden layer with three processing nodes employs hyperbolic tangent activation. The architecture completes with a single-node output layer featuring linear activation. Fig. 2 illustrates the complete PID-NN controller structure.

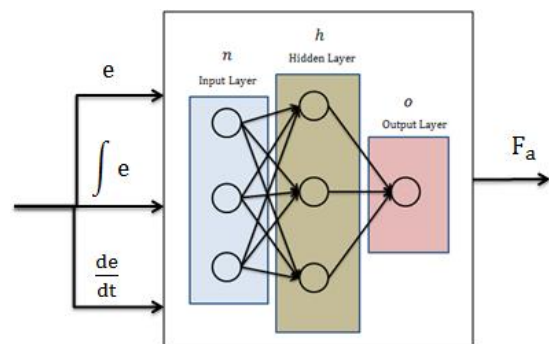


Fig. 2. Layout of PID-NN controller

Specifically, the PID-NN controller's control law is presented by:

hidden layer h_j :

$$h_j = \tanh\left(\sum_{i=1}^3 w_i n_i\right), j = 1,2,3 \quad (38)$$

output layer (o):

$$o = \sum_{j=1}^3 w_j h_j \quad (39)$$

B. PI-PD Controller

In this part, a PI-PD controller is presented as an upgraded form of the conventional PID controller. This new configuration enhances control efficiency in unstable processes and increases resilience to changes in system parameters [38]. Fig. 3 shows the diagram of the PI-PD control structure [39]-[40]. The PI-PD controller's control law (u) can be obtained by [41]:

$$u = K_{p1}e + K_i \int e - \left(K_{p2}y + K_d \frac{dy}{dt}\right) \quad (40)$$

In this context, e corresponds to the error and y to the process output. The gains are defined as follows: K_{p1} and K_{p2} are the proportional terms, K_i is the integral term, and K_d is the derivative term.

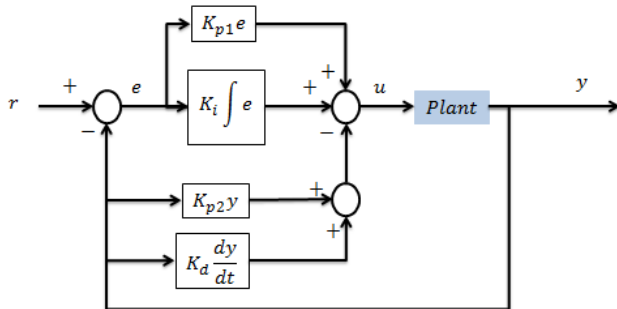


Fig. 3. Block diagram of PI-PD controller

The simplicity of the PI-PD controller's structure does not diminish the importance of its tuning process. For the controller to function efficiently, the best configuration of its parameters must be accurately determined.

IV. HONEY BADGER ALGORITHM

Optimization algorithms help identify the best possible solution from multiple available options for specific problems. These methods serve as crucial instruments across various practical applications, particularly in engineering and industrial sectors to improve the quality of the solution [42]-[44]. In this direction, the choice of design variables for the controller significantly influences its performance [45]-[46]. Many researchers in the field of controller design adopt optimization techniques to identify suitable controller parameters. The Honey Badger Algorithm (HBA), originally proposed by Hashim et al. in 2022, will be discussed in this study [47]. The honey badger detects food sources in the surroundings by moving slowly and by using its keen sense

of smell. It first employs excavation to discover the prey approximate place prior catching it. It may drill up to fifty trenches in a forty-kilometer radius or more in a single day while looking for food. Conversely, while the honeyguide bird can pinpoint beehives, it lacks the ability to reach the honey inside. This interdependence fosters a mutualistic partnership—the bird directs the badger to the hive location, enabling both species to benefit, and the badger uses its long claws to open them, allowing both to benefit from their collaborative effort [47].

The honey badger's approaches to seeking food act as a guide for the HBA. In the natural world, this substantial technique for seeking food serve is considered as an inspiration for the HBA. In nature, this resilient mammal employs two key hunting techniques to locate nourishment. Employs two key hunting techniques to locate nourishment: tracking the honeyguide bird or using the sense of smell when looking for prey. The digging method is a term used for the first method and the honey method to the second. While in the digging method, the honey badger discovers its prey through its keen sense of smell. After arriving, it examines the surrounding area to determine the ideal place for excavating and gathering the prey. The honey badger performs alongside with the honeyguide bird in the honey strategy, which directs it directly to beehives so it can locate and approach the hive successfully.

Modeled after the honey badger's natural hunting strategies, the HBA mimics this creature's food-searching patterns. Its success largely stems from maintaining an optimal balance between broad search capabilities and targeted resource utilization, which is crucial for efficient search processes. HBA incorporates dynamic search strategies, allowing it to tackle complex optimization problems with numerous local optima. By preserving sufficient population diversity throughout the search process, HBA can explore a wide range of areas within the solution space, making it well-suited for addressing challenging optimization tasks. As a global optimization method, HBA incorporates dual search strategies—exploration and exploitation—to efficiently navigate solution spaces. See Algorithm 1 for the detailed pseudocode.

The population of potential solutions in HBA can be seen as follows: The population of probable solutions.

$$= \begin{bmatrix} X_{11} & X_{12} & X_{13} & \dots & X_{1D} \\ X_{21} & X_{22} & X_{23} & \dots & X_{2D} \\ \dots & \dots & \dots & \dots & \dots \\ X_{n1} & X_{n2} & X_{n3} & \dots & X_{nD} \end{bmatrix} \quad (41)$$

i th position of the honey badger

$$X_i = [X_i^1, X_i^2, \dots, X_i^D]$$

The algorithmic steps are given as follows:

Step 1: The period for initialization. Using Equation (42), determine the very first population size (N) of honey badgers and their localities.

$$X_i = LB_i + R_1 \times (UB_i - LB_i), \quad (42)$$

where LB_i and UB_i are the upper and lower limits of the search area, X_i is i th location of honey badger position that

represents a probable solution in a population, and R_1 is an arbitrary number between zero and one.

Step 2: Describe the intensity (I), which depends on how concentrated and how close the prey is to the honey badger. I_i represents the strength of the scent emitted by the prey. A stronger scent indicates a closer or more prominent target, prompting faster movement; if the scent is weaker, the movement slows down this behavior follows the Inverse Square Law [48].

$$I_i = R_2 \times \frac{S}{4\pi D_i^2}, \quad (43)$$

where R_2 is a random number between 0 and 1, S is source strength or concentration strength given by $S = (X_i - X_{i+1})^2$, and $D_i = X_{prey} - X_i$.

Algorithm 1 Pseudo code of HBA.

Set parameters $T_{maximum}$, β , c .
The population is Initialized with random positions.
The cost function of each position x_i is evaluated and assign to F_i , $i \in [1, 2, \dots, N]$.
The best position x_{prey} is saved and assigned the fitness to f_{prey} .

While $T \leq T_{maximum}$ **do**
 Update the decreasing factor α using Eq. (44).
 for $i = 1$ to N **do**
 Using Eq. (43) to calculate the intensity I_i
 if $R < 0.5$ **then**
 Using Eq. (45) to update the position X_{new}
 else
 Using Eq. to update the position X_{new}
 end if
 Evaluate new position and assign to F_{new} .
 if $F_{new} \leq F_i$ **then**
 Set $X_i = X_{new}$ and $F_i = F_{new}$.
 end if
 if $F_{new} \leq F_{prey}$ **then**
 Set $X_{prey} = X_{new}$ and $F_{prey} = F_{new}$.
 end if
 end for
end while Stop criteria satisfied.
Print X_{prey} and $F_{X_{prey}}$

Step 3: Modify the density factor (α). From exploration to exploitation, it guarantees a seamless transition by managing the time-varying randomization process. By using Eq. (44) to modify the decreasing factor α , which lowers with repetitions, randomization can be reduced over time [49]:

$$\alpha = c \times \exp\left(\frac{-T}{T_{maximum}}\right), \quad (44)$$

where $T_{maximum}$ = maximum number of iterations and c is a constant ≥ 1 (i.e. $c=1$).

Step 4: To prevent the algorithm from converging to a local optimum, it uses a control flag (F) that alters the direction of the search. This mechanism improves the algorithm's exploratory behavior, enabling the agents to more effectively scan the solution space in search of optimal results.

Step 5: Updating the agents' positions X_{new} where this process is divided into two parts named "digging phase" and "honey phase". Eq. (45) provides an illustration of the cardioid motion.

$$X_{new} = X_{prey} + F \times \beta \times I \times X_{prey} + F \times R_3 \times \alpha \times D_i \times |\cos(2\pi R_4) \times [1 - \cos(2\pi R_5)]| \quad (45)$$

X_{prey} represents the position of the prey, which corresponds to the globally best solution identified up to the current iteration. $\beta \geq 1$ (i.e. $\beta = 1$) is the ability of the honey badger to get food. R_3 , R_4 , and R_5 are three different random numbers between 0 and 1. The variable F functions as a flag to switch the search direction and is calculated using Eq. (46):

$$F = \begin{cases} 1 & \text{if } R_6 \leq 0.5 \\ -1 & \text{else} \end{cases} \quad (46)$$

where R_6 is a random number between zero and one.

The interaction described by Eq. (47) simulates how a honey badger is guided by a honeyguide bird toward a beehive.

$$X_{new} = X_{prey} + F \times R_7 \times \alpha \times D_i \quad (47)$$

Where the random number R_7 ranges between zero and one.

V. NUMERICAL SIMULATIONS

This section presents simulation findings based on a MATLAB program to assess the efficiency of the PI-PD and PID-NN controllers to control the dual-link robot framework. The controller aim is to ensure that the dual-link robot framework angular position follow a step input. The simulation is performed using the characteristics of the dual-link robot arm framework, which is described by Equations (34), (35), (36) and (37). Table I displays the system parameters [1]-[5].

TABLE I. KEY PHYSICAL PARAMETERS OF THE TWO-LINK ROBOTIC ARM

Parameters	Values
First link mass (M_1)	1 kg
Second link mass (M_2)	1 kg
First link length (L_1)	1 m
Second link length (L_2)	1 m
Gravitational acceleration (g)	9.81 m/s ²

To achieve optimum controller efficiency, the weights of each controller are modified through the HBA. The Integral Time of Absolute Errors (ITAE) index can be found using equation (48) [50]-[54] in the optimization process.

$$ITAE = \int_{tt=0}^{tt=t_{sim}} tt|e(t)|dt \quad (48)$$

where tt is the time and t_{sim} is the total simulation time. Table II presents the configuration settings used for the Honey Badger Algorithm (HBA).

The time response of the angular angles θ_1 and θ_2 when the system is exposed to a unit step input is illustrated in Fig. 4. Measuring the settling time (t_s), steady state error (e_{ss}), maximum overshoot, and ITAE index is the way the response is assessed. Table III lists these specifications' numerical

values for the two responses. It is evident from Fig. 4 that the two controllers are capable of successfully stabilizing and controlling the system with zero e_{ss} , and zero overshoot response. In terms of t_s and the ITAE index, the dynamics of the PID-NN controller perform better than the dynamics of the PI-PD controller. Table III shows that the settling time t_s improves with the use of the PID-NN controller. Compared to the PI-PD controller, the times for θ_1 and θ_2 responses decrease from 2.3 sec and 1.2 sec to 0.8 sec and 0.55 sec, respectively. This means that the value of t_s is improved by 65.21% and 54.17% for θ_1 and θ_2 respectively. A further improvement is observed in the ITAE index, which drops from 59.19 for θ_1 and 29.3 for θ_2 using the PI-PD controller, to 11.6 for both responses under the PID-NN controller. This means that the value of the ITAE index is improved by 80.4% and 60.4% for θ_1 and θ_2 respectively.

TABLE II. CONFIGURATION SETTINGS FOR THE HONEY BADGER OPTIMIZATION

Parameters	Values
Number of individuals (N_{pop})	25
Maximum iterations (T_{max})	50
Coefficient β	1
Coefficient c	1

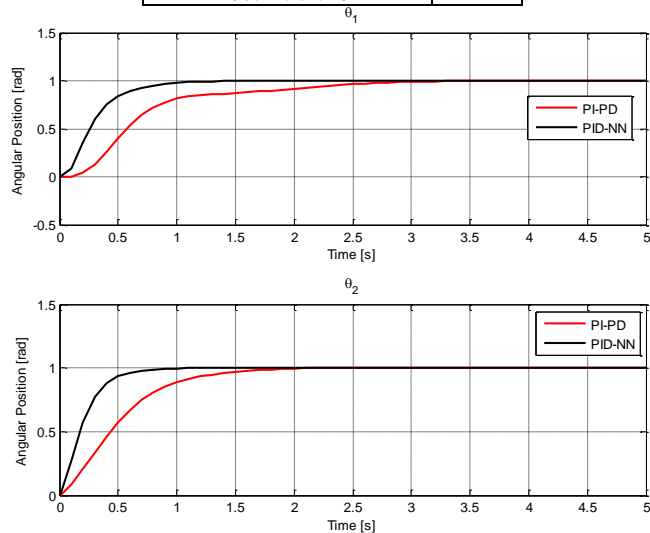


Fig. 4. Response of θ_1 and θ_2 for unit step input

TABLE III. SPECIFICATION PERFORMANCES OF SYSTEM WITHOUT DISTURBANCE

Controller	θ	Settling Time (s)	Error Steady State (rad)	Maximum Overshoot (%)	ITAE
PI-PD	θ_1	2.3	0	0	59.19
	θ_2	1.2	0	0	29.3
PD-NN	θ_1	0.8	0	0	11.6
	θ_2	0.55	0	0	11.6

To evaluate the two controllers against load variation, it was assumed that the value of the first mass has increased by 20% and the value of the second mass has increased by 50% after 4 seconds of simulation. The same designed variables of the controllers were used in the simulation. The time response for the controlled system under mass variation is shown in Fig. 5. The system's recovery time and the percentage of undershoot have been adopted to evaluate the performance of

the system as given in Table IV. Fig. 5 highlights that the PID-NN controller outperforms the PI-PD controller in the mass variation scenario. For example, Table III shows that the recovery time is reduced from 3.25 sec and 2.24 sec for θ_1 and θ_2 response respectively in the case of the PI-PD controller to 1.3 sec and 0 sec for θ_1 and θ_2 response respectively in the case of the PID-NN controller. This means that the value of the recovery time is improved by 60% and 100% for θ_1 and θ_2 respectively. Additionally, the maximum undershoot index is reduced from 20% and 8.7% for θ_1 and θ_2 response respectively in the case of the PI-PD controller to 4% and 2% for θ_1 and θ_2 response respectively in the case of the PID-NN. This means that the maximum undershoot is improved by 80% and 77% for θ_1 and θ_2 respectively. Additionally, the ITAE index's value has declined. from 215.1 and 106.87 for θ_1 and θ_2 response respectively in the case of PI-PD controller to 21.188 and 21.188 for θ_1 and θ_2 response respectively in the case of PID-NN. This means that the value of ITAE index is improved by 89.96% and 80.17% for θ_1 and θ_2 respectively. The comprehensive overview of the performance of both controller structures indicates that the PID-NN outperforms of the PI-PD across the two considered scenarios.

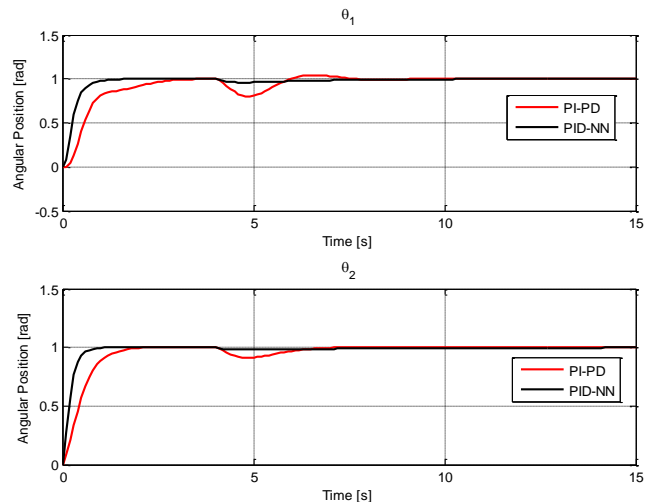


Fig. 5. Response of θ_1 and θ_2 for unit step input with mass variation

TABLE IV. SPECIFICATION PERFORMANCES OF THE SYSTEM WITH MASS VARIATION

Controller	θ	Recovery Time (s)	Maximum Undershoot (%)	ITAE
PI-PD	θ_1	3.25	20%	215.1
	θ_2	2.24	8.7%	100.7
PID-NN	θ_1	1.3	4%	82.6
	θ_2	0	2%	82.6

VI. CONCLUSION

This paper presents controlling the two-link robot system based on two control structures named PI-PD and PD-PID controllers. The behavior of the system was modeled using Lagrange mechanics. HBA was used to tune the controllers' design parameters in order to guarantee that each controller operated at its optimal performance. According to the simulation results, which were obtained using a MATLAB program, the two controllers optimized by the HBA were able to successfully stabilize and regulate the two angular

positions of the robot system with a 0% error steady state and 0% overshoots. The outcomes also demonstrate that the PID-NN controller works faster than the PI-PD controller in terms of lowering the ITAE index and settling time. Based on the numerical results, the settling time has been improved by 65.21% and 54.17% for θ_1 and θ_2 respectively whereas the ITAE index has been improved by 80.4% and 60.4% for θ_1 and θ_2 respectively. Additionally, the PID-NN controller shows an outstanding improvement in reducing the impact of load variation. Based on the results, undershoot was improved by 80% and 77% for θ_1 and θ_2 respectively whereas the ITAE index has been improved by 89.96% and 80.17% for θ_1 and θ_2 respectively. For future work of this research, another swarm optimization could be applied for selecting the controller's development configurations. Another extension of this study could be by applying a hybrid nonlinear controller.

REFERENCES

- [1] M. Baccouch and S. Dodds, "A two-link robot manipulator: Simulation and control design," *International Journal of Robotic Engineering*, vol. 5, no. 2, pp. 1-17, 2020.
- [2] N. Dersarkissian, R. Jia, and D. L. Feitosa, "Control of a two-link robotic arm using fuzzy logic," *2018 IEEE International Conference on Information and Automation (ICIA)*, pp. 481-486, 2018.
- [3] J. Velagic M. Hebibovic, and B. Lacevic, "On-Line Identification of a Robot Manipulator Using Neural Network with an Adaptive Learning Rate," *IFAC Proceedings*, vol. 38, no. 1, pp. 403-408, 2005.
- [4] C. Li-jie, "Research on the nonlinear dynamical behavior of double pendulum," *2011 International Conference on Mechatronic Science, Electric Engineering and Computer (MEC)*, pp. 1637-1640, 2011.
- [5] A. A. Mohammed and A. Eltayeb, "Dynamics and control of a two-link manipulator using PID and sliding mode control," *2018 International Conference on Computer, Control, Electrical, and Electronics Engineering (ICCCEEE)*, pp. 1-5, 2018.
- [6] E. H. Guechi, S. Bouzoualegh, Y. Zennir, and S. Blažič, "MPC control and LQ optimal control of a two-link robot arm: A comparative study," *Machines*, vol. 6, no. 3, p. 37, 2018.
- [7] A. Bendimrad, A. El Amrani, and B. El Amrani, "Optimization of the Performances of a Two-Joint Robotic Arm using Sliding Mode Control," *International Journal of Automotive and Mechanical Engineering*, vol. 19, no. 2, pp. 9634-9646, 2022.
- [8] Y. Long, J. You, Y. Huang, Z. Chen, and M. Shi, "Robust Variable Structure PID Controller for Two-Joint Flexible Manipulator," *International Conference on Computing, Control and Industrial Engineering*, pp. 133-144, 2023.
- [9] Y. Shen, "Robotic trajectory tracking control system based on fuzzy neural network," *Measurement: Sensors*, vol. 31, p. 101006, 2024.
- [10] H. Al-Khazraji, "Comparative study of whale optimization algorithm and flower pollination algorithm to solve workers assignment problem," *International Journal of Production Management and Engineering*, vol. 10, no. 1, pp. 91-98, 2022.
- [11] F. R. Yaseen, M. Q. Kadhim, H. Al-Khazraji, and A. J. Humaidi, "Decentralized Control Design for Heating System in Multi-Zone Buildings Based on Whale Optimization Algorithm," *Journal Européen des Systèmes Automatisés*, vol. 57, no. 4, pp. 981-989, 2024.
- [12] H. Al-Khazraji, S. Khlil, and Z. Alabacy, "Industrial picking and packing problem: Logistic management for products expedition," *Journal of Mechanical Engineering Research and Developments*, vol. 43, no. 2, pp. 74-80, 2020.
- [13] F. R. Al-Ani, O. F. Lutfy, and H. Al-Khazraji, "Optimal Synergetic and Feedback Linearization Controllers Design for Magnetic Levitation Systems: A Comparative Study," *Journal of Robotics and Control (JRC)*, vol. 6, no. 1, pp. 22-30, 2025.
- [14] H. Al-Khazraji, K. Al-Badri, R. Al-Majeez, and A. J. Humaidi, "Synergetic control design based sparrow search optimization for tracking control of driven-pendulum system," *Journal of Robotics and Control (JRC)*, vol. 5, no. 5, pp. 1549-1556, 2024.
- [15] S. Khlil, H. Al-Khazraji, and Z. Alabacy, "Solving assembly production line balancing problem using greedy heuristic method," *IOP Conference Series: Materials Science and Engineering*, vol. 745, no. 1, pp. 1-7, 2020.
- [16] H. Al-Khazraji, A. R. Nasser, and S. Khlil, "An intelligent demand forecasting model using a hybrid of metaheuristic optimization and deep learning algorithm for predicting concrete block production," *IAES International Journal of Artificial Intelligence*, vol. 11, no. 2, pp. 649-657, 2022.
- [17] F. R. Yaseen and H. Al-Khazraji, "Optimized Vector Control Using Swarm Bipolar Algorithm for Five-Level PWM Inverter-Fed Three-Phase Induction Motor," *International Journal of Robotics and Control Systems*, vol. 5, no. 1, pp. 333-347, 2025.
- [18] H. AL-Khazraji, C. Cole, and W. Guo, "Optimization and simulation of dynamic performance of production-inventory systems with multivariable controls," *Mathematics*, vol. 9, no. 5, p. 568, 2021.
- [19] A. K. Ahmed, H. Al-Khazraji, and S. M. Raafat, "Optimized PI-PD Control for Varying Time Delay Systems Based on Modified Smith Predictor," *International Journal of Intelligent Engineering & Systems*, vol. 17, no. 1, pp. 331-342, 2024.
- [20] H. Al-Khazraji, R. M. Naji, and M. K. Khashan, "Optimization of sliding mode and back-stepping controllers for AMB systems using gorilla troops algorithm," *Journal Européen des Systèmes Automatisés*, vol. 57, no. 2, pp. 417-424, 2024.
- [21] R. Al-Majeez, K. Al-Badri, H. Al-Khazraji, and S. M. Ra'afat, "Design of A Backstepping Control and Synergetic Control for An Interconnected Twin-Tanks System: A Comparative Study," *International Journal of Robotics and Control Systems*, vol. 4, no. 4, pp. 2041-2054, 2024.
- [22] H. Al-Khazraji, W. Guo, and A. J. Humaidi, "Improved cuckoo search optimization for production inventory control systems," *Serbian Journal of Electrical Engineering*, vol. 21, no. 2, pp. 187-200, 2024.
- [23] M. A. AL-Ali, O. F. Lutfy, and H. Al-Khazraj, "Comparative Study of Various Controllers Improved by Swarm Optimization for Nonlinear Active Suspension Systems with Actuator Saturation," *International Journal of Intelligent Engineering & Systems*, vol. 17, no. 4, pp. 870-881, 2024.
- [24] Z. N. Mahmood, H. Al-Khazraji, and S. M. Mahdi, "PID-based enhanced flower pollination algorithm controller for drilling process in a composite material," *Annales de Chimie. Sci. des Matériaux*, vol. 47, no. 2, pp. 91-96, 2023.
- [25] R. M. Naji, H. Dulaimi, and H. Al-Khazraji, "An optimized PID controller using enhanced bat algorithm in drilling processes," *Journal Européen des Systèmes Automatisés*, vol. 57, no. 3, pp. 767-772, 2024.
- [26] A. K. Ahmed and H. Al-Khazraji, "Optimal control design for propeller pendulum systems using gorilla troops optimization," *Journal Européen des Systèmes Automatisés*, vol. 56, no. 4, pp. 575-582, 2023.
- [27] H. Al-Khazraji, C. Cole, and W. Guo, "Analysing the impact of different classical controller strategies on the dynamics performance of production-inventory systems using state space approach," *Journal of Modelling in Management*, vol. 13, no. 1, pp. 211-235, 2018.
- [28] M. A. Al-Ali, O. F. Lutfy, and H. Al-Khazraj, "Investigation of optimal controllers on dynamics performance of nonlinear active suspension systems with actuator saturation," *Journal of Robotics and Control (JRC)*, vol. 5, no. 4, pp. 1041-1049, 2024.
- [29] A. J. Humaidi, T. M. Kadhim, S. Hasan, I. K. Ibraheem, and A. T. Azar, "A Generic Izhikevich-Modelled FPGA-Realized Architecture: A Case Study of Printed English Letter Recognition," *2020 24th International Conference on System Theory, Control and Computing (ICSTCC)*, pp. 825-830, 2020.
- [30] A. J. Humaidi and T. M. Kadhim, "Spiking versus traditional neural networks for character recognition on FPGA platform," *Journal of Telecommunication, Electronic and Computer Engineering*, vol. 10, no. 3, pp. 109-115, 2018.
- [31] A. J. Humaidi and T. M. Kadhim, "Recognition of Arabic Characters using Spiking Neural Networks," *2017 International Conference on Current Trends in Computer, Electrical, Electronics and Communication (CTCEEC)*, pp. 7-11, 2017.
- [32] A. Al-Jodah, S. J. Abbas, A. F. Hasan, A. J. Humaidi, A. S. Al-Obaidi, A. A. Al-Qassar, and R. F. Hassan, "PSO-based optimized neural network PID control approach for a four wheeled omnidirectional

- mobile robot," *International Review of Applied Sciences and Engineering*, vol. 14, no. 1, pp. 58–67, 2023.
- [33] A. M. Abood, A. R. Nasser, and H. Al-Khazraji, "Predictive maintenance of electromechanical systems based on enhanced generative adversarial neural network with convolutional neural network," *IAES International Journal of Artificial Intelligence (IJ-AI)*, vol. 12, no. 4, pp. 1704–1712, 2023.
- [34] H. Ziad, A. Al-Dujaili, and A. J. Humaidi, "Electrical faults classification in permanent magnet synchronous motor using ResNet neural network," *International Review of Applied Sciences and Engineering*, vol. 15, no. 3, pp. 355–364, 2024.
- [35] M. I. Mansoor, H. M. Tuama, and A. J. Humaidi, "Application of correlation-based recurrent neural network in porosity prediction for petroleum exploration," *Engineering Research Express*, vol. 7, no. 1, p. 015241, 2025.
- [36] M. Y. Hasan, D. J. Kadhim, and A. J. Humaidi, "Prediction of electricity-consumption and residential bills based on artificial neural network," *International Review of Applied Sciences and Engineering*, vol. 16, no. 1, pp. 142–152, 2025.
- [37] O. A. M. López, A. M. López, and J. Crossa, "Multivariate statistical machine learning methods for genomic prediction," *Springer Nature*, p. 691, 2022.
- [38] N. Tan, "Computation of stabilizing PI-PD controllers," *International Journal of Control, Automation and Systems*, vol. 7, pp. 175–184, 2009.
- [39] M.M. Ozyetkin, C. Onat, and N. Tan, "PI-PD controller design for time delay systems via the weighted geometrical center method," *Asian Journal of Control*, vol. 22, no. 5, pp. 1811–1826, 2020.
- [40] F. Alyoussef, I. Kaya, and A. Akrad, "Robust PI-PD Controller Design: Industrial Simulation Case Studies and a Real-Time Application," *Electronics*, vol. 13, no. 17, p. 3362, 2024.
- [41] F. Peker and I. Kaya, "Identification and real time control of an inverted pendulum using PI-PD controller," *2017 21st International Conference on System Theory, Control and Computing (ICSTCC)*, pp. 771–776, 2017.
- [42] T. R. Farshi, "Battle royale optimization algorithm," *Neural Computing and Applications*, vol. 33, no. 4, pp. 1139–1157, 2021.
- [43] H. Al-Khazraji, S. Khilil, and Z. Alabacy, "Cuckoo search optimization for solving product mix problem," *IOP Conference Series: Materials Science and Engineering*, vol. 1105, no. 1, p. 012016, 2021.
- [44] H. Al-Khazraji, S. Khilil, and Z. Alabacy, "Solving mixed-model assembly lines using a hybrid of ant colony optimization and greedy algorithm," *Engineering and Technology Journal*, vol. 40, no. 1, pp. 172–180, 2022.
- [45] H. Al-Khazraji and L. T. Rasheed, "Performance evaluation of pole placement and linear quadratic regulator strategies designed for mass-spring-damper system based on simulated annealing and ant colony optimization," *Journal of Engineering*, vol. 27, no. 11, pp. 15–31, 2021.
- [46] H. Al-Khazraji, C. Cole, and W. Guo, "Multi-objective particle swarm optimisation approach for production-inventory control systems," *Journal of Modelling in Management*, vol. 13, no. 4, pp. 1037–1056, 2018.
- [47] F. A. Hashim, E. H. Houssein, K. Hussain, M. S. Mabrouk, and W. Al-Atabany, "Honey Badger Algorithm: New metaheuristic algorithm for solving optimization problems," *Mathematics and Computers in Simulation*, vol. 192, pp. 84–110, 2022.
- [48] D. J. Kapner, T. S. Cook, E. G. Adelberger, J. H. Gundlach, B. R. Heckel, C. D. Hoyle, and H. E. Swanson, "Tests of the gravitational inverse-square law below the dark-energy length scale," *Physical review letters*, vol. 98, no. 2, p. 021101, 2007.
- [49] M. H. Khan, A. Ulasyar, A. Khattak, H. S. Zad, M. Alsharif, A. A. Alahmadi, and N. Ullah, "Optimal sizing and allocation of distributed generation in the radial power distribution system using honey badger algorithm," *Energies*, vol. 15, no. 16, p. 5891, 2022.
- [50] F. R. Al-Ani, O. F. Lutfy, and H. Al-Khazraji, "Optimal Backstepping and Feedback Linearization Controllers Design for Tracking Control of Magnetic Levitation System: A Comparative Study," *Journal of Robotics and Control (JRC)*, vol. 5, no. 6, pp. 1888–1896, 2024.
- [51] M. Q. Kadhim, F. R. Yaseen, H. Al-Khazraji, and A. J. Humaidi, "Application of Terminal Synergetic Control Based Water Strider Optimizer for Magnetic Bearing Systems," *Journal of Robotics and Control (JRC)*, vol. 5, no. 6, pp. 1973–1979, 2024.
- [52] H. Al-Khazraji, "Optimal Design of a Proportional-Derivative State Feedback Controller Based on Meta-Heuristic Optimization for a Quarter Car Suspension System," *Mathematical Modelling of Engineering Problems*, vol. 9, no.2, pp. 575–582, 2022.
- [53] Z. N. Mahmood, H. Al-Khazraji, and S. M. Mahdi, "Adaptive control and enhanced algorithm for efficient drilling in composite materials," *Journal Européen des Systèmes Automatisés*, vol. 56, no. 3, pp. 507–512, 2023.
- [54] H. Al-Khazraji, K. Al-Badri, R. Almajeez, and A. J. Humaidi, "Synergetic control-based sea lion optimization approach for position tracking control of ball and beam system," *International Journal of Robotics and Control Systems*, vol. 4, no. 4, pp. 1547–1560, 2024.